Glauber cross sections for arbitrary excitation of ground-state hydrogen by electron and proton impact

S. K. Sur and N. C. Sil

Department of Theoretical Physics, Indian Association for the Cultivation of Science, Jadavpur, Calcutta 700 032, India

(Received 20 August 1979)

The Glauber scattering amplitude for $1s$-nlm excitations of hydrogen by charged particle impact is reduced to a form numerically computable for arbitrary values of n, l, and m. The increasing number of repeated parametric differentiations appearing in earlier methods with the increase of n is replaced in our method by a single contour integration, which is especially useful for large-n states. In addition, whereas the available closed-form expressions would involve the calculation of a large number of hypergeometric functions as l and m increase for a given n, the present integral form involves only one hypergeometric function for any n, l, and m. The asymptotic form of the $1s$-nlm amplitude as $n\to\infty$ is also presented. The procedure is applied for studying the $1s\to ns$ ($n = 3$, 4, 10, and ∞) and $1s\to np$ ($n = 3$, 4, and ∞) excitations of hydrogen by electron and proton impact. Tabular results of the cross sections are presented for differential and integrated cross sections in e^--H collisions and for integrated cross sections in H^+-H collisions. The qualitative features observed earlier for low ns and np excitations are found to exist also for $n \geq 3$ excitations. The $1s\to ns$ and $1s\to np$ cross sections obey an n^{-3} law asymptotically as $n^{-2}\to 0$, which is in conformity with the analytical results obtained quite generally for $1s\to nlm$ excitations. For proton impact $1s\to 3p$ excitations, the Glauber results are in excellent agreement with a recent 34-state calculation. A unified graphical representation of various normalized cross sections above some specific energy is presented, whence a knowledge of the high-energy Born cross sections for any $1s\to ns$ or $1s\to np$ excitation suffices to determine the absolute Glauber cross sections for the process.

I. INTRODUCTION

Highly excited states of atomic or ionic targets and their collisional formation in hot astrophysical or laboratory plasmas have attracted considerable interest in the literature in recent years.[1-3] Theoretical studies of the high-lying transitions in such systems can be performed using classical or semiclassical methods.[1] However, such methods are not applicable for investigating high excitation of atoms from the ground or low-lying states, where exact quantum-mechanical cross sections should be calculated. Quantal calculations, on the other hand, suffer from serious computational difficulties whenever the principal quantum number n of any of the initial and final states approaches large values. This may be the reason for the lack of exact quantum theoretical data for high atomic excitation prevailing in the literature so far. Very recently, however, Sil and co-workers[3] have been able to find a general procedure to eliminate the relevant computational troubles for hydrogenlike targets and have successfully applied it to calculate the cross sections for various $1s$-nlm excitations in such targets by charged particle impact using the first Born approximation (FBA) and other related first-order methods. Extension of this procedure[3] to the investigation of similar processes within the framework of more reliable theories hence appears worthwhile.

The conventional Glauber approximation[4] (GA) provides such a theoretical framework for studying inelastic scattering of structureless charged particles from neutral atomic targets at intermediate and high incident energies. For direct excitation of atomic hydrogen, specifically, the success of the Glauber theory during the last decade has been remarkable.[5-7] In the region of validity of the first Born approximation the integrated Glauber cross sections approach the Born values, as expected. At lower energies, on the other hand, the Glauber results are distinctly superior to the FBA values when compared with experiment and can predict the physical features in the cross-section-energy curve, which are obtainable only from much more arduous theoretical calculations. Furthermore, the GA-predicted angular distributions for inelastic scattering of intermediate energy electrons from hydrogen at angles less than 90° show very good agreement with observed results.[5] This has been confirmed also for the scattering of protons from hydrogen in a very recent experiment by Park *et al.*[8] They measure the angular differential cross sections for excitation of hydrogen atoms to the $n=2$ level and obtain remarkable agreement with the Glauber results at angles less than 10^{-3} rad in the center-of-mass (c.m.) system. In view of the above success, the reliability of the Glauber theory for studying inelastic processes in charged-particle–neutral-hydrogen collisions at intermediate and high energies can hardly be overemphasized. On general theoretical grounds, however, the Glauber theory has its limitations when extended towards an incident velocity range $v_i < 1$ a.u. or to wide angle-inelastic scattering, and care must be taken not to extrapolate it too far at such

regions.

The Glauber cross sections for various discrete excitations of ground-state hydrogen have been studied by several authors.[2,6,9-12] However, only a few works have been concerned with the case of arbitrary transitions of hydrogen.[2,13,14] Considering later applications of the methods employed to cases of more complicated atomic targets, the work of Thomas and Gerjuoy[13] has remained as an important one. They have reduced the GA-scattering amplitude for $1s$-ns and $1s$-np excitations of hydrogen to closed forms. These expressions are particularly suited for studying the limiting behavior of the cross sections at high energy or small momentum transfer and are easily computable as well for low excitations from the ground state. Formal extension of this method[13] to the case of arbitrary nlm-$n'l'm'$ transitions has been recently performed by Toshima,[2] who has applied it to calculate the GA cross sections for some of the relatively high-lying transitions in hydrogen. On the other hand, Thomas and Franco[7] have been able to obtain the $1s$-nlm Glauber scattering amplitude for hydrogen in a very compact form in connection with a relatively recent work on the Coulomb modifications of the conventional Glauber approximation. Kumar and Srivastava[14] have also suggested a procedure for evaluating the Glauber amplitudes for arbitrary excitation of hydrogen from the ground or low-lying states, which involves an infinite integration with products of hypergeometric functions occurring in the integrand.

All the methods of reducing the Glauber scattering amplitude for arbitrary transitions in hydrogen discussed above suffer from the common computational difficulty mentioned earlier when these are employed to study large-n-changing transitions. More specifically, the trouble develops from the customary procedure of generating higher excitation amplitudes through repeated parametric differentiations. This gives rise to a huge number of hypergeometric functions in the amplitude expression making calculations extremely troublesome. The various recurrence relations satisfied by the hypergeometric functions may be exploited to reduce the final number of such functions, but that too is a very combersome and laborious process. Indeed, Gerjuoy and Thomas[5] have observed that the appearance of a very large number of hypergeometric functions limit the usefulness of the method of Thomas and Gerjuoy[13] for large n. Toshima, in his actual calculations, also observed his method unsuitable for $n,\ n' \gtrsim 15$. These facts have led us to search for a useful alternative method of calculating the Glauber scattering amplitude so as to be applicable for high excitations of hydrogen from the ground state. We have briefly discussed in an earlier work (Sur and Sil[15]) how the repeated differentiations in cases of large values of n can be eliminated from the final expression of the scattering amplitude. The details of the derivations are given in the present paper, where, in addition, we are now able to further simplify the procedure for arbitrary values of l and m.

In the present paper, we reduce the Glauber scattering amplitude for arbitrary $1s$-nlm transitions in hydrogen and apply it for studying $1s$-ns and $1s$-np excitations by electron and proton impact. The details of the derivations and the appropriate numerical methods of calculating the $1s$-nlm amplitudes are discussed in Secs. II and III. In Sec. IV we give the limiting asymptotic forms of the amplitudes as $n \to \infty$. Section V covers the special cases of $1s$-ns and $1s$-np transitions, while in subsequent Sec. VI we present and discuss the electron and proton impact cross section results for various discrete s and p excitations as well as the corresponding limiting asymptotic values.

II. AN INTEGRAL FORM OF THE $1s \to nlm$ GLAUBER AMPLITUDE FOR HYDROGEN

For direct collisional excitation of a hydrogen atom from an initial state $\Psi_i(\vec{r})$ to a final state $\Psi_f(\vec{r})$ by the impact of a structureless particle of charge Z_i and relative velocity $\vec{v}_i$, the Glauber scattering amplitude in the center-of-mass (c.m.) system is given by (using atomic units throughout)

$$F(i \to f; \vec{q}) = \frac{iK_i}{2\pi} \int \Psi_f^*(\vec{r}) \Gamma(\vec{b}, \vec{r}) \Psi_i(\vec{r}) e^{i\vec{q}\cdot\vec{b}} d^2b\, d\vec{r}, \tag{1}$$

with

$$\Gamma(\vec{b}, \vec{r}) = 1 - (|\vec{b} - \vec{s}|/b)^{2i\eta}. \tag{2}$$

Here $\eta = -Z_i/v_i$, $\vec{q} = (\vec{K}_i - \vec{K}_f)$ is the momentum transfer vector, $\vec{K}_i$ and $\vec{K}_f$ are the incident and final relative momenta, and $\vec{s}$ denotes the projection of $\vec{r}$, the position vector of the bound electron onto the plane containing $\vec{q}$ and $\vec{b}$.

The atomic wave functions can be conveniently quantized along the direction of the Glauber path integration as usual.[9-13] Thus, we can write for the ground $1s$ state and an arbitrary nlm state of the target hydrogen atom,

$$\Psi_{1s}(\vec{r}) = N_1 e^{-r} \tag{3}$$

and

$$\Psi_{nlm}(\vec{r}) = N_{nl} e^{-r/n} r^l L_{n+l}^{2l+1}(2r/n) Y_{lm}(\hat{r}), \tag{4}$$

where

$$N_1 = \frac{1}{\sqrt{\pi}}, \quad N_{nl} = -\frac{1}{n}\left(\frac{2}{n}\right)^{l+1}\left(\frac{(n-l-1)!}{(n+l)!^3}\right)^{1/2},$$

$L_b^a(x)$ is the associated Laguerre polynomial of order $b-a$, and $Y_{lm}(\hat{r})$ represents the spherical harmonic.

Instead of using the conventional expansion of L_b^a given by Schiff[16] or the alternative form in terms of the confluent hypergeometric functions employed by Thomas and Gerjuoy,[13] we now follow Sil and co-workers[3] to use an integral representation for the associated Laguerre function[17]:

$$L_b^a(x) = (-1)^{a+1}\frac{i}{\pi}\frac{b}{2^{a+1}}\oint_C dz\,(z-1)^{a-1}\left(\frac{z+1}{z-1}\right)^b \times \exp\left(-\frac{x}{2}(z-1)\right), \tag{5}$$

where a and b are integers. The integral on the right-hand side is to be performed along a closed contour C on the complex z plane, which encloses the singularity at $z=1$ of the integrand function. Inserting the expression (5) in Eq. (4), we can write the product of the wave functions to be substituted in Eq. (1) as

$$\Psi_{nlm}^*(\vec{r})\Psi_{1s}(\vec{r}) = -\frac{i}{\pi}N_1 N_{nl}\frac{(n+l)!}{2^{2l+2}}r^l Y_{lm}^*(\hat{r}) \times \oint_C dz\,(z-1)^{2l}\left(\frac{z+1}{z-1}\right)^{n+l} e^{-\lambda r}, \tag{6}$$

with $\lambda = 1 + z/n$, whence the Glauber scattering amplitude given by Eq. (1) becomes

$$F(1s \to nlm;\vec{q}) = A_{nl}K_i \times \oint_C dz\left(\frac{z^2-1}{n^2}\right)^l\left(\frac{z+1}{z-1}\right)^n g_{lm}(\lambda,\vec{q}), \tag{7}$$

where

$$g_{lm}(\lambda,\vec{q}) = \int e^{-\lambda r}r^l\Gamma(\vec{b},\vec{r})e^{i\vec{q}\cdot\vec{b}}Y_{lm}^*(\hat{r})d^2b\,d\vec{r} \tag{8}$$

and

$$A_{nl} = (N_1 N_{nl}/8\pi^2)(n+l)!\,(n/2)^{2l}. \tag{9}$$

In writing Eq. (7) we have interchanged the order of integration over z with the integrations over $\vec{b}$ and $\vec{r}$ on the assumption that these latter integrations are well-defined and convergent for each and every value of z on the contour C, which includes the singularity of the integrand function at $z=1$ only.

Introducing now the generating function

$$I_{lm}(\lambda,\vec{q}) = \int e^{-\lambda r}r^{l-1}\Gamma(\vec{b},\vec{r})e^{i\vec{q}\cdot\vec{b}}Y_{lm}^*(\hat{r})d^2b\,d\vec{r}, \tag{10}$$

we can write

$$g_{lm}(\lambda,\vec{q}) = -(\partial/\partial\lambda)I_{lm}(\lambda,\vec{q}), \tag{11}$$

whence Eq. (7) gives

$$F(1s \to nlm;\vec{q}) = -A_{nl}K_i \times \oint_C dz\left(\frac{z^2-1}{n^2}\right)^l\left(\frac{z+1}{z-1}\right)^n\frac{\partial I_{lm}(\lambda,\vec{q})}{\partial\lambda}. \tag{12}$$

The integral on the right-hand side can be immediately simplified through integration by parts, giving

$$n\left[\left(\frac{z^2-1}{n^2}\right)^l\left(\frac{z+1}{z-1}\right)^n I_{lm}(\lambda,\vec{q})\right]_C - \oint_C dz\left\{\left(\frac{\partial}{\partial\lambda}\right)\left[\left(\frac{z^2-1}{n^2}\right)^l\left(\frac{z+1}{z-1}\right)^n\right]\right\}I_{lm}(\lambda,\vec{q}), \tag{13}$$

where we have used the relation $(\partial/\partial\lambda) = n(\partial/\partial z)$. The first term in (13) vanishes since the contour C is a closed one, so that Eq. (12) becomes

$$F(1s \to nlm;\vec{q}) = A_{nl}K_i \oint_C dz\frac{\partial\Phi_{nl}(\lambda)}{\partial\lambda}I_{lm}(\lambda,\vec{q}), \tag{14}$$

where the function $\Phi_{nl}(\lambda)$ has a dependence on $z/n = \lambda - 1$ rather than on z and is defined via

$$\Phi_{nl}(\lambda) = \left(\frac{z^2-1}{n^2}\right)^l\left(\frac{z+1}{z-1}\right)^n. \tag{15}$$

The troublesome λ differentiation of the generating functions appearing in earlier methods[2,7,13] are thus eliminated, and Eq. (14) already gives an integral form suitable for application in case of arbitrary n excitations of hydrogen from the ground state, provided of course, the contour integral can be efficiently evaluated. This has been confirmed by actual numerical computations from Eq. (14) for the $1s$-ns excitation in e^--H collisions. For the corresponding generating function $I_{00}(\lambda,\vec{q})$, we have used the final reduced form of the analogous function given by Thomas and Gerjuoy.[13] As mentioned earlier, the method of Thomas and Gerjuoy has been generalized by Toshima[2] for arbitrary nlm-$n'l'm'$ excitations. This procedure can be used for the reduction of $I_{lm}(\lambda,\vec{q})$ given by Eq. (10) to closed-form expressions which can then be substituted in Eq. (14) for subsequent numerical work. But this route does not appear promising because of the appearance of multiple summations involving hypergeometric functions in the expression for $I_{lm}(\lambda,\vec{q})$ as l,m increase. Such complications result from the authors'[2,13] use of cylindrical coordinates for $\vec{r}$ in the reduction procedure, when the Legendre function P_l^m oc-

curring in the spherical harmonic Y_{lm} need be expanded in a power series.[2]

On the other hand, Thomas and Franco[7] employ spherical polar coordinates for $\vec{r}$ and by exploiting the properties of $Y_{lm}(\hat{r})$ obtain a very compact form for the generating function [cf. Eq. (B3) of Ref. 7]:

$$I_{lm}(\lambda, \vec{q}) = B_{lm}(\eta) Y^*_{lm}(\tfrac{1}{2}\pi, \varphi_q) q^{-l-4} \left[\left(\frac{-\partial}{\partial u} \right)^{1+(l-|m|)/2} h_{lm}(u) \right] \tag{16}$$

for $l \geq 0$, where φ_q is the azimuthal angle of $\vec{q}$ in the plane containing $\vec{q}$ and $\vec{b}$,

$$h_{lm}(u) = u^{-i\eta}\, {}_2F_1((l+|m|)/2 - i\eta,\ 1+|m|-i\eta;\ 1+|m|;\ -u), \tag{17}$$

with $u = \lambda^2/q^2$ and

$$B_{lm}(\eta) = 16\pi^2 i\eta (2i)^l \frac{\Gamma(1+i\eta)\Gamma((l+|m|)/2 - i\eta)\Gamma(1+|m|-i\eta)}{\Gamma(1-i\eta)\Gamma(1+|m|)}. \tag{18}$$

As we show in the following, Eqs. (16) and (17) especially suit our procedure allowing some very useful simplifications which are not possible with the form obtainable from the methods of Refs. 2 and 13. The generating function $I_{lm}(\lambda, \vec{q})$ for hydrogen follows as a special case of the corresponding function for hydrogenlike ions in the Coulomb-modified Glauber approximation of Thomas and Franco.[7]

Substituting for $I_{lm}(\lambda, \vec{q})$ from Eq. (16) into (14), we have

$$F(1s \to nlm; \vec{q}) = A_{nl} B_{lm}(\eta) K_i Y^*_{lm}(\tfrac{1}{2}\pi, \varphi_q) q^{-l-4} \oint_C dz \frac{\partial \Phi_{nl}(\lambda)}{\partial \lambda} \left[\left(-\frac{\partial}{\partial u} \right)^{1+(l-|m|)/2} h_{lm}(u) \right]. \tag{19}$$

The partial differentiations appearing in the second term of the integral can be effectively transferred to the first one through repeated application of integration by parts, as in the analogous case of Eqs. (12) through (14). This yields

$$F(1s \to nlm; \vec{q}) = A_{nl} B_{lm}(\eta) 2^{-1-(l-|m|)/2} n K_i Y^*_{lm}(\tfrac{1}{2}\pi, \varphi_q) q^{-2-|m|} \oint_C \frac{dz}{n} \lambda \left[\left(\frac{1}{\lambda} \frac{\partial}{\partial \lambda} \right)^{2+(l-|m|)/2} \Phi_{nl}(\lambda) \right] h_{lm}(u). \tag{20}$$

On substitution for $\Phi_{nl}(\lambda)$, $h_{lm}(u)$, A_{nl}, and $B_{lm}(\eta)$ from Eqs. (15), (17), (8), and (18), respectively, in Eq. (20), the full expression for the Glauber scattering amplitude for $1s$-nlm transitions in hydrogen, after proper simplification, becomes

$$F(1s \to nlm; \vec{q}) = C_{nl} D_{lm}(\eta) Y^*_{lm}(\tfrac{1}{2}\pi, \varphi_q) q^{2i\eta - |m| - 2} K_i \oint_C \frac{dz}{n} \lambda^{1-2i\eta} \left\{ \left(\frac{1}{\lambda} \frac{\partial}{\partial \lambda} \right)^{2+(l-|m|)/2} \left[\left(\frac{z^2-1}{n^2} \right)^l \left(\frac{z+1}{z-1} \right)^n \right] \right\}$$
$$\times {}_2F_1[(l+|m|)/2 - i\eta,\ 1+|m|-i\eta;\ 1+|m|;\ -\lambda^2/q^2] \tag{21}$$

for $l \geq 0$, where

$$C_{nl} = n^{-3/2} \left[\prod_{r=0}^{l} \left(1 - \frac{r^2}{n^2} \right) \right]^{-1/2}, \tag{22a}$$

$$D_{lm}(\eta) = -2^{1-(l-|m|)/2} i^{l+1} \frac{\eta}{\sqrt{\pi}} \frac{\Gamma(1+i\eta)\Gamma((l+|m|)/2 - i\eta)\Gamma(1+|m|-i\eta)}{\Gamma(1-i\eta)\Gamma(1+|m|)}. \tag{22b}$$

Several points about Eq. (21) may now be noted. First of all, Eq. (21) is valid for all $n \geq 1$. Thus, the Glauber ($1s$-$1s$) elastic amplitude is also computable from Eq. (21). However, it is well known that the elastic Glauber predictions are unreliable and we are interested here in direct excitations, for which $n \geq 2$. The greatest advantage of Eq. (21) is that it involves only one hypergeometric function for any set of values of nlm. The present form supersedes our previous work[15] based on the methods of Thomas and Gerjuoy,[13] and of Toshima,[2] in which one would not be able to avoid the computation of a large number of hypergeometric functions with increasing values of l, m. Thus, Eq. (21) amounts to a still greater reduction of computational labor than that achieved earlier,[15] especially for high nlm excitations from the ground state. The contour integral in Eq. (21) can be analytically evaluated by the method of residues to yield the formula of Thomas and Franco,[7] which is useful in computing the excitation amplitudes for low excitations from the ground state, where neither of n, l, m is large. In this respect, another great advantage of the amplitude expression (21) is that, for a given set of values of l, m all the n-excitation cross sections can be obtained from a common computer program. Efficient evaluation of the integral in Eq. (21) depends, however, on proper choice of the contour C, which we now proceed to discuss.

III. CHOICE OF CONTOUR AND NUMERICAL METHOD

Equation (21) can be written in the form

$$F(1s \to nlm; \vec{q}) = C_{nl} K_i f_{nlm}(\vec{q}), \tag{23}$$

where

$$f_{nlm}(\vec{q}) = D_{lm}(\eta) Y^*_{lm}(\tfrac{1}{2}\pi, \varphi_q) q^{2i\eta - |m| - 2} \times \oint_C \frac{dz}{n} \lambda^{1-2i\eta} \left[\left(\frac{1}{\lambda} \frac{\partial}{\partial \lambda} \right)^{2+(l-|m|)/2} \Phi_{nl}(\lambda) \right] {}_2F_1[(l+|m|)/2 - i\eta, 1+|m| - i\eta; 1+|m|; -\lambda^2/q^2], \tag{24}$$

C_{nl} and $D_{lm}(\eta)$ being given by Eqs. (22).

The integrand in Eq. (24) is, on inspection, found to have singularities at $z=1$, $-n$, $-n(1 \pm iq)$, and ∞, the first of which at $z=1$ arises from the term in $\Phi_{nl}(\lambda)$ and happens to be the only singularity which should be enclosed by the contour C, the second at $z=-n$ occurs because of the term $\lambda^{1-2i\eta}$, while the rest are the singularities of the hypergeometric function. Thus the distance of the nearest singular point ($z=-n$) of the integrand function in (24) from the point $z=1$ increases with n. Furthermore, it should be noted that since $\lambda = 1 + z/n$, the integrand function has an implicit z dependence through z/n. Both of these facts can be exploited to our advantage provided we choose the contour C to be a circle having its center at the origin ($z=0$) and with a radius proportional to n. Thus we take

$$C\colon\ z = ane^{i\theta},\quad a < 1,\quad n \geq 2. \tag{25}$$

The value of the proportionality constant a should be adjusted such that numerical calculation of the hypergeometric functions can be done in an efficient manner. We find that this can be achieved by taking $a = 0.7$. From Eq. (24), we have

$$f_{nlm}(\vec{q}) = iaD_{lm}(\eta) Y^*_{lm}(\tfrac{1}{2}\pi, \varphi_q) q^{2i\eta - |m| - 2} \times \int_0^{2\pi} d\theta\, e^{i\theta} \lambda^{1-2i\eta} \left[\left(\frac{1}{\lambda} \frac{\partial}{\partial \lambda} \right)^{2+(l-|m|)/2} \Phi_{nl}(\lambda) \right] {}_2F_1[(l+|m|)/2 - i\eta, 1+|m| - i\eta; 1+|m|; -\lambda^2/q^2], \tag{26}$$

for $n \geq 2$, where $\lambda = 1 + ae^{i\theta}$ is now independent of n. The n dependence of $f_{nlm}(\vec{q})$ thus occurs only through the term $\Phi_{nl}(\lambda)$. As shown in the following, in the limit of very large n, $\Phi_{nl}(\lambda)$, and hence, $f_{nlm}(\vec{q})$ become independent of n. The asymptotic n dependence of the Glauber amplitude is thus contained solely in the term C_{nl} given by Eq. (22a).

The integral in Eq. (26) can be evaluated by employing the usual Gauss-Legendre quadrature method, preferably after breaking the range of integration into suitable intervals.

IV. ASYMPTOTIC LIMIT OF $f_{nlm}(\vec{q})$ AS $n \to \infty$

Let us put $\gamma = n/z = 1/(\lambda - 1)$. It is then easy to verify that

$$[(z+1)/(z-1)]^n_{n\to\infty} = \exp(2\gamma) + O(1/n^2), \tag{27}$$

and

$$[(z^2-1)/n^2]^l_{n\to\infty} = \gamma^{-2l} + O(1/n^2), \tag{28}$$

so that from Eq. (15) we have

$$\lim_{n\to\infty} \Phi_{nl}(\lambda) = \gamma^{-2l} e^{2\gamma} + O(1/n^2), \tag{29}$$

where l, m are finite. Since λ is independent of n by our choice of the contour C, we have

$$\lim_{n\to\infty} \left[\left(\frac{1}{\lambda} \frac{\partial}{\partial \lambda} \right)^p \Phi_{nl}(\lambda) \right] = \left(\frac{1}{\lambda} \frac{\partial}{\partial \lambda} \right)^p (\gamma^{-2l} e^{2\gamma}). \tag{30}$$

On substitution from (30) in (26) we find that the integral in (26) approaches a value indepent of n as $n^{-2} \to 0$, the limiting value of $f_{nlm}(\vec{q})$ being given by

$$f^0_{lm}(\vec{q}) = [f_{nlm}(\vec{q})]_{n\to\infty} = iaD_{lm}(\eta) Y^*_{lm}(\tfrac{1}{2}\pi, \varphi_q) q^{2i\eta - |m| - 2} \times \int_0^{2\pi} d\theta\, e^{i\theta} \lambda^{1-2i\eta} \left[\left(\frac{1}{\lambda} \frac{\partial}{\partial \lambda} \right)^{2+(l-|m|)/2} (\gamma^{-2l} e^{2\gamma}) \right] {}_2F_1[(l+|m|)/2 - i\eta, 1+|m| - i\eta; 1+|m|; -\lambda^2/q^2], \tag{31}$$

where l, m are finite. As mentioned earlier, the asymptotic n dependence of the amplitude expression (23) is obtained from the term C_{nl}. From Eq. (22a), we readily have

$$(C_{nl})_{n\to\infty} = n^{-3/2}. \tag{32}$$

Thus the Glauber scattering amplitude for $1s$-nlm excitation of hydrogen shows an asymptotic $n^{-3/2}$ dependence in the limit $n\to\infty$.

Equation (31), along with Eq. (23), provides a useful form for obtaining the asymptotic limit of the $1s$-nlm Glauber amplitudes.

V. SPECIAL CASES

The Glauber scattering amplitudes for the transitions $1s\to ns$ and $1s\to np$ have been reduced by Thomas and Gerjuoy.[13] As discussed earlier, the closed form expressions derived by Thomas and Gerjuoy involve increasing number of repeated parametric differentiations of hypergeometric functions as n increases. We have discussed elsewhere[15] how these differentiations can be avoided from the final expression of the scattering amplitude. However, this method[15] also would involve calculation of large number of hypergeometric functions as l, m increase for a specific value of n. Our present form of the Glauber scattering amplitude given by Eqs. (23), (26), and (31) are free from this latter type of trouble also. To show this explicitly for the cases $1s\to ns$ and $1s\to np$, we give the corresponding expressions for the scattering amplitude in the following.

Inserting $l=m=0$ in Eqs. (23) and (26) we have, after some simplification,

$$F(1s\to ns;\vec{q}) = n^{-3/2}K_i f_{ns}(\vec{q}), \tag{33a}$$

$$f_{ns}(\vec{q}) = \frac{2a\eta}{\pi}\Gamma(1+i\eta)\Gamma(-i\eta)q^{2i\eta-2} \times \int_0^{2\pi} d\theta\, e^{i\theta}\lambda^{-2-2i\eta}\left(\frac{z+1}{z-1}\right)^n\left(\frac{n^2}{z^2-1}\right)\left(1+\frac{2\lambda^2n^2}{z^2-1}\right){}_2F_1(-i\eta,1-i\eta;1;-\lambda^2/q^2), \tag{33b}$$

while the corresponding asymptotic form as $n\to\infty$ (l,m being finite) is obtained from Eqs. (23) and (31):

$$[F(1s\to ns;\vec{q})]_{n\to\infty} = n^{-3/2}K_i f^0_{00}(\vec{q}), \tag{34a}$$

$$f^0_{00}(\vec{q}) = \frac{2a\eta}{\pi}\Gamma(1+i\eta)\Gamma(-i\eta)q^{2i\eta-2} \times \int_0^{2\pi} d\theta\, e^{2\gamma+i\theta}\gamma^2(2\gamma^2+4\gamma+3)\lambda^{-2-2i\eta}{}_2F_1(-i\eta,1-i\eta;1;-\lambda^2/q^2). \tag{34b}$$

Equations (33) and (34) are only alternative forms of the corresponding expressions for $1s$-ns Glauber scattering amplitudes given in our earlier work.[15] Indeed, by exploiting the recurrence relations of the hypergeometric functions and by integrating once by parts, the earlier expressions of Ref. 15 can be rederived from Eqs. (33) and (34).

For $1s$-np, the term $Y^*_{lm}(\frac{1}{2}\pi, \varphi_q)$ in Eqs. (26) and (31) make them vanish for $l=1$, $m=0$ ($1s\to np_0$ transition), which is already known as the selection rule for Glauber amplitude. The nonvanishing ($1s\to np_{\pm1}$) amplitudes are obtained by putting $l=1$, $m=\pm1$ in Eqs. (23), (26), and (31) as

$$F(1s\to np_{\pm1};\vec{q}) = \left(\frac{n^2}{n^2-1}\right)^{-1/2} n^{-3/2}K_i f_{np_{\pm1}}(\vec{q}), \tag{35a}$$

$$f_{np_{\pm1}}(\vec{q}) = \frac{2\sqrt{6}\,\eta}{\pi}(ia)\Gamma(1+i\eta)\Gamma(2-i\eta)e^{\mp i\varphi_q}q^{2i\eta-3} \times \int_0^{2\pi} d\theta\, e^{i\theta}\left(\frac{z+1}{z-1}\right)^n\left(\frac{n^2}{z^2-1}\right)\lambda^{-2-2i\eta}{}_2F_1(1-i\eta,2-i\eta;2-\lambda^2/q^2). \tag{35b}$$

The asymptotic form of Eq. (35) as $n\to\infty$ (but l, m finite) is given by

$$[F(1s\to np_{\pm1};\vec{q})]_{n\to\infty} = n^{-3/2}K_i f^0_{1,\pm1}(\vec{q}), \tag{36a}$$

$$f^0_{1,\pm1}(\vec{q}) = \frac{2\sqrt{6}\,\eta}{\pi}\,\frac{i}{a}\Gamma(1+i\eta)\Gamma(2-i\eta)e^{\mp i\varphi_q}q^{2i\eta-3}\int_0^{2\pi} d\theta\, e^{2\gamma-i\theta}\lambda^{2-2i\eta}{}_2F_1(1-i\eta,2-i\eta;2;-\lambda^2/q^2). \tag{36b}$$

The expressions (35) and (36) are simpler than those given earlier[15] in that each involves only one hypergeometric function in the integrand.

Scaled cross section

The center-of-mass differential cross sections for $1s \to nlm$ excitations are given by

$$\frac{d\sigma(1s \to nlm)}{d\Omega} = (K_f/K_i)\left|F(1s \to nlm; \vec{q})\right|^2$$

$$= C_{nl}^2 K_i K_f \left|f_{nlm}(\vec{q})\right|^2 , \qquad (37)$$

on substitution from Eq. (23). In view of the discussion following Eq. (26) and that in Sec. IV, it is convenient to introduce the scaled differential cross sections:

$$\frac{d\bar{\sigma}(1s \to nlm)}{d\Omega} = C_{nl}^{-2} \frac{d\sigma(1s \to nlm)}{d\Omega}$$

$$= n^3 \left[\prod_{r=0}^{l}\left(1 - \frac{r^2}{n^2}\right)\right] \frac{d\sigma(1s \to nlm)}{d\Omega} , \qquad (38)$$

where we have substituted for C_{nl} from Eq. (22a). Then, from Eq. (37), we have

$$\frac{d\bar{\sigma}(1s \to nlm)}{d\Omega} = K_i K_f \left|f_{nlm}(\vec{q})\right|^2 . \qquad (39)$$

Since the Glauber amplitudes are evaluated by quantizing along a direction which lies in the scattering plane and is perpendicular to $\vec{q}$ at each $\vec{K}_i$ and $\vec{K}_f$, Eqs. (37)–(39) are dependent on the quantization axis which changes with scattering angle. However, if the magnetic sublevels are summed over, the sum is independent of quantization axis. Thus the $1s \to nl$ differential cross sections, summed over the magnetic sublevels, becomes

$$\frac{d\sigma(1s \to nl)}{d\Omega} = \frac{K_f}{K_i} \sum_m \left|F(1s \to nlm; \vec{q})\right|^2 \qquad (40)$$

and

$$\frac{d\bar{\sigma}(1s \to nl)}{d\Omega} = K_i K_f \sum_m \left|f_{nlm}(\vec{q})\right|^2 . \qquad (41)$$

The total $1s \to nl$ cross section can be obtained from the customary relation

$$\sigma(1s \to nl) = 2\pi \int_{-1}^{1} \frac{d\sigma(1s \to nl)}{d\Omega}\, d\gamma , \qquad (42)$$

where γ is the cosine of the angle of scattering in the c.m. system.

VI. RESULTS AND DISCUSSION

We have obtained numerical results of the Glauber cross sections for $1s$-ns and $1s$-np excitations of hydrogen by electron and proton impact collisions. For the two projectiles, we have prepared two general computer programs (PROG 1 and PROG 2) for calculating the scaled s- and p-excitation cross sections for arbitrary discrete n

TABLE I. Scaled differential cross sections $[d\bar{\sigma}(1s \to ns)/d\Omega]$ (a_0^2/sr) at various electron energies for the process: $e^- + \mathrm{H}(1s) \to e^- + \mathrm{H}(ns)$.

Scattering angle (deg)	50 eV $n=3$	50 eV $n=4$	50 eV $n=10$	50 eV $n\to\infty$	100 eV $n=3$	100 eV $n=4$	100 eV $n=10$	100 eV $n\to\infty$	200 eV $n=3$	200 eV $n=4$	200 eV $n=10$	200 eV $n\to\infty$
0.0	0.582(+1)[a]	0.458(+1)	0.357(+1)	0.341(+1)	0.717(+1)	0.565(+1)	0.444(+1)	0.424(+1)	0.690(+1)	0.543(+1)	0.425(+1)	0.407(+1)
6.7	0.394(+1)	0.322(+1)	0.261(+1)	0.251(+1)	0.349(+1)	0.292(+1)	0.242(+1)	0.234(+1)	0.261(+1)	0.221(+1)	0.185(+1)	0.179(+1)
15.4	0.148(+1)	0.129(+1)	0.112(+1)	0.109(+1)	0.103(+1)	0.933	0.835	0.817	0.492	0.466	0.438	0.432
24.2	0.494	0.457	0.418	0.411	0.247	0.237	0.227	0.225	0.636(−1)	0.622(−1)	0.609(−1)	0.607(−1)
33.0	0.160	0.153	0.146	0.145	0.627(−1)	0.606(−1)	0.587(−1)	0.584(−1)	0.149(−1)	0.141(−1)	0.134(−1)	0.133(−1)
41.7	0.605(−1)	0.578(−1)	0.554(−1)	0.549(−1)	0.259(−1)	0.243(−1)	0.228(−1)	0.226(−1)	0.659(−2)	0.615(−2)	0.573(−2)	0.566(−2)
50.5	0.340(−1)	0.313(−1)	0.289(−1)	0.285(−1)	0.156(−1)	0.144(−1)	0.134(−1)	0.132(−1)	0.362(−2)	0.338(−2)	0.314(−2)	0.309(−2)
59.3	0.258(−1)	0.233(−1)	0.211(−1)	0.207(−1)	0.106(−1)	0.979(−2)	0.904(−2)	0.891(−2)	0.217(−2)	0.202(−2)	0.188(−2)	0.186(−2)
68.1	0.214(−1)	0.194(−1)	0.175(−1)	0.172(−1)	0.743(−2)	0.691(−2)	0.640(−2)	0.631(−2)	0.138(−2)	0.129(−2)	0.120(−2)	0.119(−2)
76.8	0.179(−1)	0.163(−1)	0.149(−1)	0.146(−1)	0.537(−2)	0.501(−2)	0.466(−2)	0.459(−2)	0.932(−3)	0.870(−3)	0.810(−3)	0.799(−3)
85.6	0.149(−1)	0.137(−1)	0.126(−1)	0.124(−1)	0.400(−2)	0.374(−2)	0.348(−2)	0.343(−2)	0.660(−3)	0.617(−3)	0.574(−3)	0.567(−3)

[a] $x(\pm y) \equiv x \times 10^{\pm y}$.

TABLE II. Scaled differential cross sections $[d\bar{\sigma}(1s \to np)/d\Omega]$ (a_0^2/sr) at various electron energies for the process: $e^- + \mathrm{H}(1s) \to e^- + \mathrm{H}(np)$.

Scattering angle (deg)	50 eV $n=3$	50 eV $n=4$	50 eV $n\to\infty$	100 eV $n=3$	100 eV $n=4$	100 eV $n\to\infty$	200 eV $n=3$	200 eV $n=4$	200 eV $n\to\infty$
0.0	0.102(+3)[a]	0.798(+2)	0.592(+2)	0.263(+3)	0.206(+3)	0.153(+3)	0.584(+3)	0.457(+3)	0.338(+3)
3.3	0.846(+2)	0.677(+2)	0.514(+2)	0.140(+3)	0.116(+3)	0.921(+2)	0.123(+3)	0.106(+3)	0.886(+2)
6.7	0.533(+2)	0.466(+2)	0.357(+2)	0.510(+2)	0.451(+2)	0.385(+2)	0.280(+2)	0.258(+2)	0.232(+2)
11.4	0.244(+2)	0.218(+2)	0.186(+2)	0.148(+2)	0.139(+2)	0.128(+2)	0.524(+1)	0.523(+1)	0.517(+1)
16.6	0.100(+2)	0.938(+1)	0.863(+1)	0.407(+1)	0.408(+1)	0.404(+1)	0.871	0.923	0.982
23.4	0.317(+1)	0.316(+1)	0.311(+1)	0.802	0.846	0.897	0.978(−1)	0.106	0.117
32.1	0.772	0.806	0.844	0.125	0.134	0.147	0.118(−1)	0.127(−1)	0.136(−1)
50.1	0.800(−1)	0.841(−1)	0.895(−1)	0.109(−1)	0.114(−1)	0.121(−1)	0.100(−2)	0.104(−2)	0.110(−2)
69.9	0.201(−1)	0.209(−1)	0.219(−1)	0.229(−2)	0.240(−2)	0.252(−2)			
87.9	0.838(−2)	0.878(−2)	0.926(−2)	0.806(−3)	0.844(−3)	0.890(−3)			

[a] $x(\pm y) \equiv x \times 10^{\pm y}$.

states. These programs have been checked by running them for $n=2$ and 3 states, when the existing Glauber results for $2s$, $2p$ (Refs. 9–12), $3s$, and $3p$ (Refs. 10, 12) excitations are reproduced. Separate programs (**PROG 1A** and **PROG 2A**) have been prepared for obtaining the scaled limiting asymptotic cross sections for large n. The cross section values predicted by these latter programs (**PROG 1A** and **PROG 2A**) agree to within 1% with the predictions of the corresponding earlier programs (**PROG 1** and **PROG 2**) at a value of $n=20$.

The above programs have been employed to obtain the differential and integrated Glauber cross sections for both e^--H and H^+-H collisions. The states which have been considered are $n=3$, 4, and ∞ for both $1s$-ns and $1s$-np excitations. In addition, we have run the $1s$-ns program (PROG 1) for an arbitrarily high state, viz., $n=10$, to show the usefulness of the present method. The scaled values of the differential and total cross sections are presented in Tables I–VI, while some of the results are also displayed graphically in Figs. 1–4 for convenient comparison with existing theories as well as with experiments where available. Furthermore, we give in Fig. 5 a unified graphical representation of the normalized total Glauber cross sections for both electron and proton impact collisions. These curves may be used in estimating the relative $1s$-ns and $1s$-np Glauber cross sections for any arbitrary value of $n \geq 3$.

TABLE III. Scaled total Glauber cross sections $\bar{\sigma}(1s \to ns)(10^{-1}\pi a_0^2)$ for the process: $e^- + \mathrm{H}(1s) \to e^- + \mathrm{H}(ns)$.

Energy (eV) \ n	3	4	10	∞
15	0.824	0.534	0.304	0.268
20	2.40	1.93	1.51	1.44
30	3.99	3.42	2.91	2.82
40	4.25	3.70	3.20	3.12
50	4.07	3.57	3.11	3.03
60	3.77	3.32	2.90	2.83
75	3.31	2.92	2.56	2.50
100	2.69	2.37	2.09	2.04
150	1.90	1.69	1.49	1.45
200	1.47	1.30	1.14	1.12
300	1.00	0.889	0.784	0.766
400	0.761	0.679	0.601	0.587

A. Electron impact excitation

Tables I and II contain our Glauber results of the scaled differential cross sections $(d\bar{\sigma}/d\Omega)$ for electron impact $1s$-ns and $1s$-np excitations, respectively. The results are given at a number of scattering angles for 50- 100- and 200-eV electrons. The corresponding values of the scaled total cross sections $(\bar{\sigma})$ are presented in Tables III and IV.

TABLE IV. Scaled total Glauber cross sections $\bar{\sigma}(1s \to np)(\pi a_0^2)$ for the process: $e^- + \mathrm{H}(1s) \to e^- + \mathrm{H}(np)$.

Energy (eV) \ n	3	4	∞
15	1.05	0.803	0.526
20	2.19	1.88	1.53
30	3.23	2.85	2.45
40	3.48	3.09	2.68
50	3.46	3.03	2.67
60	3.34	2.97	2.58
100	2.76	2.45	2.12
200	1.85	1.63	1.41
300	1.44	1.27	1.08
400	1.22	1.07	0.908

TABLE V. Scaled total Glauber cross sections $\bar{\sigma}(1s \to ns)(10^{-1}\pi a_0^2)$ for the process: $H^+ + H(1s) \to H^+ + H(ns)$.

Lab energy (keV) \ n	3	4	10	∞
10	4.00	3.67	3.36	3.30
15	3.29	3.00	2.74	2.69
20	3.42	3.05	2.70	2.65
30	4.46	3.91	3.41	3.33
40	5.08	4.46	3.89	3.80
50	5.26	4.62	4.04	3.94
75	4.88	4.29	3.77	3.68
100	4.26	3.78	3.30	3.22
200	2.61	2.30	2.02	1.97
300	1.84	1.62	1.42	1.39
500	1.15	1.01	0.887	0.865

1. 1s-ns transitions

The scaled $1s$-ns Glauber cross sections for $n = 3$, 4, and 10 states given in Table I are found to approach the asymptotic values (for $n \to \infty$) with increasing values of n. Indeed, the scaled cross sections for $n = 10$ and $n \to \infty$ agree to within 2% with each other except in the forward direction. These clearly reveal the asymptotic validity of the n^{-3} law of cross sections discussed in Sec. IV. A comparison of our differential Glauber predictions (not presented here) with the $1s$-$4s$ calculation of Saha *et al.*[18] using the FBA method and a polarized-Ochkur-Born (POB) approximation shows that whereas the POB cross sections are in reasonable agreement with the Glauber results at small angles, the FBA cross sections differ widely from the Glauber ones at all scattering angles. A

TABLE VI. Scaled total Glauber cross sections $\bar{\sigma}(1s \to np)(\pi a_0^2)$ for the process: $H^+ + H(1s) \to H^+ + H(np)$.

Lab energy (keV) \ n	3	4	∞
10	0.671	0.638	0.600
15	1.16	1.06	0.935
25	2.50	2.24	1.95
40	3.58	3.21	2.81
50	3.84	3.44	3.01
60	3.92	3.51	3.07
100	3.64	3.25	2.83
200	2.70	2.40	2.08
400	1.76	1.56	1.35
500	1.50	1.33	1.15

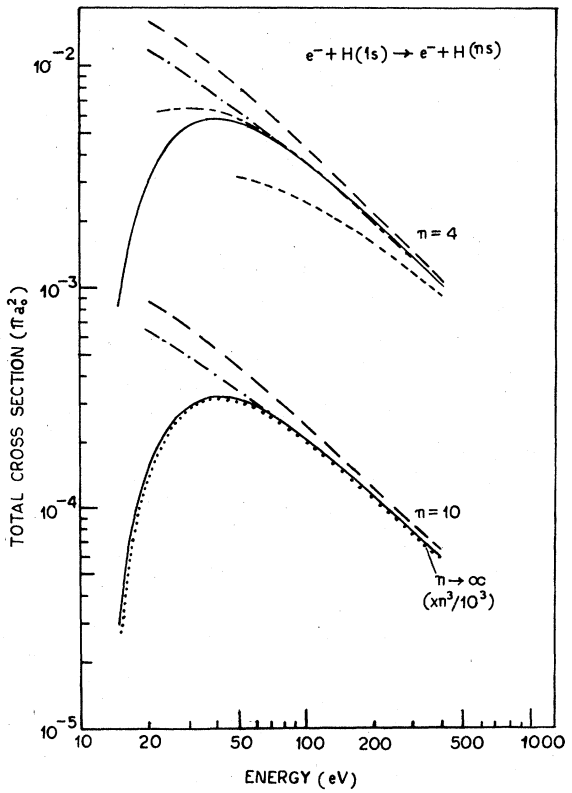

FIG. 1. Integrated cross sections for $1s \to ns$ excitation of hydrogen by electron impact. ——, present Glauber ($n = 4$, 10); ···, present Glauber ($n \to \infty$); —— - ——, McDowell *et al.* (DWPO I, $n = 4$) (Ref. 21); —— ——, Saha *et al.* (FBA, $n = 4$, 10) (Ref. 18); —— · ——, Saha *et al.* (POB, $n = 4$, 10) (Ref. 18); ---, Bayne and Heenen (SOD, $n = 4$) (Ref. 20).

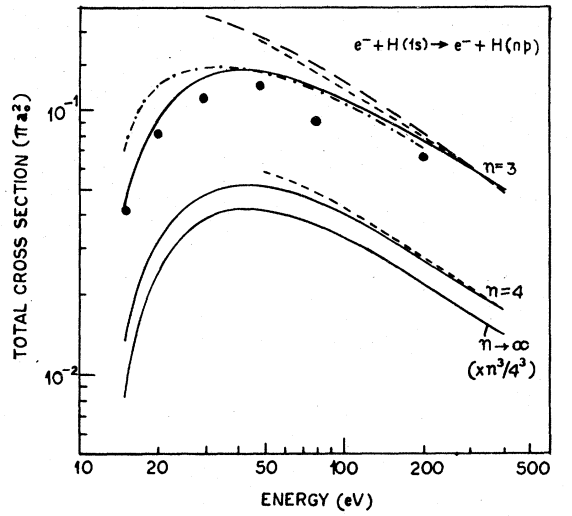

FIG. 2. Integrated cross sections for $1s \to np$ excitation of hydrogen by electron impact. ——, present Glauber ($n = 3$, 4, ∞); —— · ——, Syms *et al.* (DWPO II, $n = 3$) (Ref 19); —— ——, Saha *et al.* (FBA, $n = 3$) (Ref. 18); ---, Bayne and Heenen (SOD, $n = 3$, 4) (Ref. 23); •, experiment by Mahan *et al.* (Ref. 20).

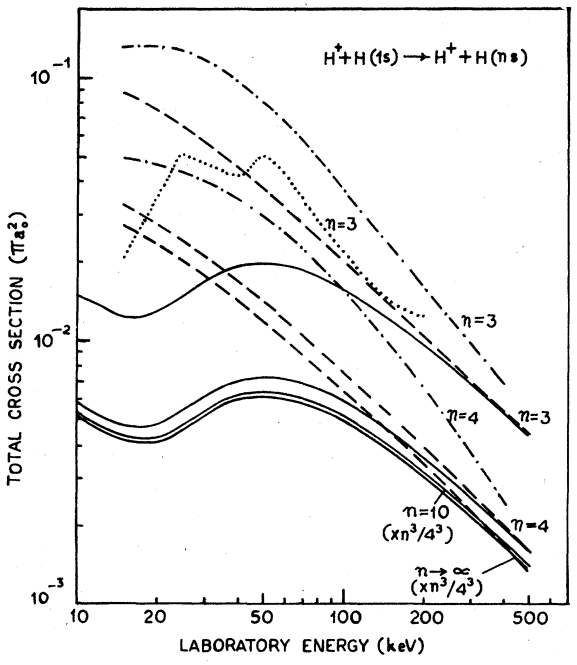

FIG. 3. Integrated cross sections for $1s \rightarrow ns$ excitation of hydrogen by proton impact. ——, present Glauber ($n = 3, 4, 10, \infty$); ···, Shakeshaft (Ref. 26); —·—, Bayne and Heenen (SOD, $n = 3, 4$) (Ref. 25); — —, Roy *et al.* (FBA, $n = 3, 4, \infty$) (Ref. 24).

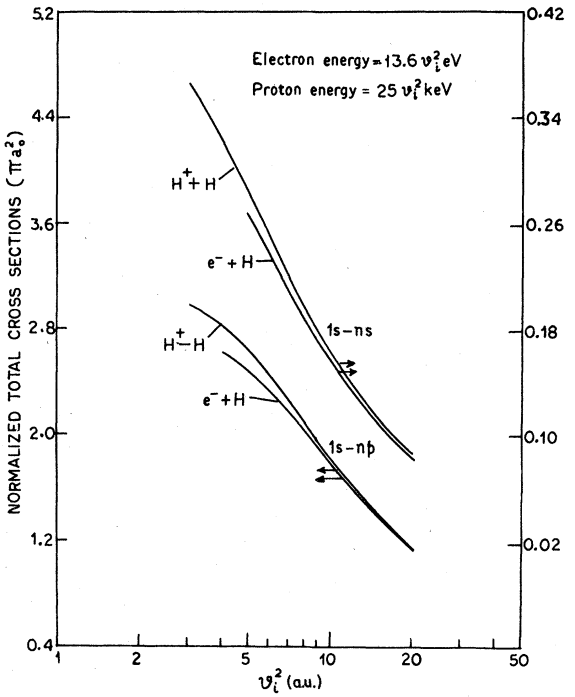

FIG. 5. Integrated Glauber cross sections for $1s \rightarrow ns$ and $1s \rightarrow np$ excitations in e^-+ H and H^++H collisions plotted against the square of the incident particle speed (v_i). Cross sections are normalized to the scaled asymptotic results.

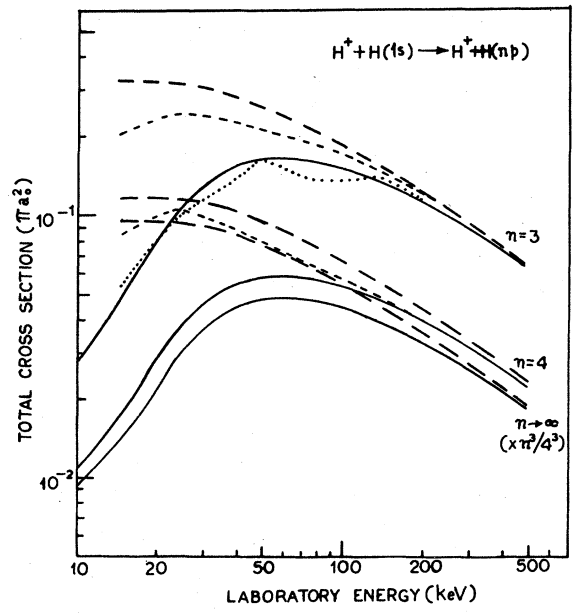

FIG. 4. Integrated cross sections for $1s \rightarrow np$ excitation of hydrogen by proton impact. ——, present Glauber ($n = 3, 4, \infty$); ···, Shakeshaft (Ref. 26); ---, Bayne and Heenen (SOD, $n = 3, 4$) (Ref. 25); — —, Roy *et al.* (FBA, $n = 3, 4, \infty$) (Ref. 24).

distorted-wave polarized orbital (DWPO II) calculation by Syms *et al.*[19] who take account of target distortion, predicts $1s$-$3s$ cross sections in good agreement with the POB and Glauber results at small scattering angles.

Considering the case of the present $1s$-ns total Glauber cross sections, it is found that for incident electron energies exceeding 30 eV, the Glauber results for the $n = 3$ state show reasonable agreement with the only available experimental data of Mahan *et al.*[20] The agreement of the present Glauber results for $n = 3$ and 4 states with the existing other theories[21,22,19] is also good except for the case of a second order diagonalization (SOD) calculation of Bayne and Heenen,[23] which appreciably underestimates all other calculations and the measurement. In Fig. 1, we plot the present electron impact total Glauber cross sections for $1s$-$4s$ and $1s$-$10s$ transitions at various incident electron energies between 15 and 400 eV. Each set of results shows a peak around 40 eV. The energy-dependence of the cross sections are similar to that obtained earlier for $1s$-$2s$ and $1s$-$3s$ transitions.[9,10] We compare the $1s$-$4s$ Glauber cross sections of Fig. 1 with the FBA and POB results of Saha *et al*,[18] as also with an earlier DWPO calculation of McDowell *et al.*,[21] in which

target distortion was neglected (DWPO I). Whereas the FBA cross sections still approach the Glauber values at the highest energies considered, the POB results coincide with the latter ones above 100 eV. Both the FBA and POB curves, however, shoot high at lower energies in complete disagreement with the Glauber curve. On the other hand, the DWPO I results are in excellent agreement with ours even up to 40 eV on the low energy side, the two results actually coinciding above 55 eV. The SOD results,[23] as in the $1s$-$3s$ case, again underestimate the predictions of all other theories in the energy range 50–400 eV. The $1s$-$10s$ Glauber cross sections of Fig. 1 are compared with the only available FBA and POB results.[18] The relative features of the calculations are similar to that observed for $1s$-$4s$ excitations. The scaled asymptotic Glauber cross sections $[(1/10)^3\bar{\sigma}(1s \to ns)]$ included in Fig. 1 are almost indistinguishable from the $1s$-$10s$ results indicating the n^{-3} dependence of cross sections in the whole energy range 15–400 eV for $n \geq 10$.

2. 1s-np transitions

As in the case of $1s$-ns transitions, the asymptotic validity of the n^{-3} law of cross sections is also observable for $1s$-np transitions from the scaled Glauber differential results of Table II. A comparison of the Glauber cross sections with DWPO II results of Syms *et al.*[19] shows that both are in good agreement at small angles.

In Fig. 2, we display the present total Glauber cross sections for electron impact $1s$-np excitations. The results for $n=3$ state have already been compared by Syms *et al.*[19] with their DWPO II calculations as well as with other theories[21,22] and the only available measurement of Mahan *et al.*[20] However, Syms *et al.* do not include the SOD calculation of Bayne and Heenen,[23] who have considered the $n=2$–4 excitations. The $n=4$ results of Bayne and Heenen happen to be the only theoretical data available for comparison with our $n=4$ results. We hence consider it worthwhile to include the $n=3$ Glauber cross sections in Fig. 2 and compare these with the SOD as well as the DWPO II and FBA[18] results. Whereas the DWPO II and Glauber calculations can predict the correct energy dependence of the measured data reasonably well throughout the range of energies considered, the SOD calculation appreciably overestimates all other results. The $1s$-$3p$ SOD cross sections, however, approach the Glauber values near 500 eV. These relative features of Glauber and SOD calculations are observed also for the $1s$-$4p$ transitions (Fig. 2). The asymptotic curve for $1s$-np excitations displayed in Fig. 2 gives the scaled values of $[(\frac{1}{4})^3\bar{\sigma}(1s \to np)]$ in the limit $n \to \infty$. The similarity of the energy dependence of the asymptotic total cross sections with those for the $n=3$ and 4 states is immediately observable.

B. Proton impact excitation

Tables V and VI contain the present integrated results of the scaled Glauber cross sections $[d\bar{\sigma}(1s \to ns, np)/d\Omega]$ in the proton energy range 10–500 keV for $1s$-ns and $1s$-np excitations, respectively.

1. 1s-ns transitions

In view of the remarkable success of the Glauber theory in predicting the correct angular distributions for inelastic scattering of intermediate energy protons from hydrogen, as observed in the recent measurement of Park *et al.*[8] for $n=2$ excitations, it may be interesting to study the $1s$-ns and $1s$-np differential Glauber cross sections in H^+-H collisions.

A graphical comparison (not presented here) of the center-of-mass differential Glauber cross sections for various n reveals that the angular dependence of the proton impact results at lower energies differ considerably from the corresponding features in electron scattering. This has already been observed by Franco and Thomas[12] for $n=2$ and 3 excitations. Thus, the differential curves for 15 keV protons exhibit minima at small scattering angles for all the $n=3$, 4, and 10 states. This feature of the differential cross sections persists in a gradually less-pronounced manner upto some higher energies, the reminiscence of which is observable as a shoulder in each of the curves for 50 keV. The FBA predicted angular differential cross sections for $1s$-$4s$ transitions[24] are seen to differ widely from the Glauber results at all energies and scattering angles.

The minima in the curves for $1s$-ns differential Glauber cross sections at proton energies around 15 keV cause a corresponding minimum in the total cross sections near 15 keV.[12] This is observable in Fig. 3, where we plot the $1s$-ns integrated Glauber cross sections against the incident proton energy for the states $n=3$, 4, 10, and ∞ and compare these with the available calculations.[25-26] Whereas the FBA[24] and Glauber results (for $n=3$, 4, and ∞) coincide near 500 keV, the SOD[25] results (for $n=3$ and 4) appreciably overestimate both the former results throughout the energy range considered. It may here be recalled that for $n=2$ excitations, first-order theories like the FBA, and distortion methods, as well as the coupled-state calculations in the impact parameter treatment neglecting charge transfer channels and the SOD

calculation,[25] do not predict any oscillation in the cross section-energy curve near 15 keV, as observed in the Glauber results (cf. Gerjuoy and Thomas[5]). Inclusion of charge transfer channels in close coupling calculations, on the other hand, do predict the oscillations in qualitative agreement with the Glauber calculations. Furthermore, the Glauber results[12] show very good agreement with the experimental measurement[27] for $1s$-$2s$ excitations even below 10 keV. This success of the Glauber theory has been considered by Franco and Thomas[12] to result from a probable implicit inclusion of coupling to charge transfer channels. However, as argued by Gerjuoy and Thomas,[5] this explanation may not be well founded in view of the inability of the Glauber cross sections to distinguish between the positive and negative charge states of an incident particle. A recent coupled-state calculation by Shakeshaft[26] using a scaled hydrogenic basis set with 34 states predicts cross sections for the $n=3$ state lying between the FBA (Ref. 24) and SOD (Ref. 25) results above 45 keV. But, whereas the FBA and SOD results go on increasing at lower energies, the coupled-state results[26] fall rapidly below 25 keV in qualitative agreement with the Glauber curve of Fig. 3. However, the coupled state results are not available below 15 keV, and the question whether the oscillation in the Glauber-predicted cross-section-energy curve near 15 keV is of a true physical nature or is just an artifact of the Glauber theory still remains undecided. Proper elucidation of this point for $n \geq 3$ states should hence await further experimental measurements, as also coupled-state calculations at low and intermediate energies. The curves for $n=10$ and ∞ of Fig. 3 give the scaled Glauber cross sections $[(\frac{1}{4})^3\bar{\sigma}(1s \to ns)]$ and, as in the case of electron impact collisions, hardly differ from each other.

2. *1s-np transitions*

The present proton impact center-of-mass Glauber differential cross sections for $1s$-np transitions for various n (not presented here) show shapes similar to those obtained earlier by Franco and Thomas.[12]

The $1s$-np total cross sections are plotted against energy in Fig. 4. The Glauber results for the $n=3$ state show excellent agreement with the 34-state results of Shakeshaft[26] throughout the energy range (15–200 keV) considered. Whereas the FBA cross sections[24] for all the $n=3$, 4, and ∞ states still approach the Glauber values at the highest energy considered, the SOD results[25] coincide with the FBA results above 200 keV for the $3p$ excitation and with the Glauber results above 150 keV for the $4p$ excitation. The energy dependence of the scaled asymptotic cross sections is similar to that observed for $1s$-$3p$ and $1s$-$4p$ transitions.

C. A unified presentation of normalized electron and proton impact total cross sections

As already known, for sufficiently high energies, the electron and proton impact total cross sections for a given direct process have the same value when considered as a function of the relative speed (v_i) of the incident particle. Our results of the total $1s$-ns and $1s$-np cross sections presented in Tables III–VI conform to these facts. If v_i is expressed in atomic units, the energy of an electron is given approximately by $13.6\, v_i^2$ eV, while that of a proton by $25\, v_i^2$ keV. Thus, a 200-eV electron has roughly the same velocity as a 400-keV proton. A comparison of the $1s$-np cross sections of Tables IV and VI at these energies shows that the results agree to within 5%.

Furthermore, as we have noted from Figs. 1–4, the integrated electron and proton impact Glauber cross sections for various values of n show similar energy dependence for either of $1s$-ns and $1s$-np transitions. This is in conformity with the discussion of Sec. IV where it has been shown that the cross sections obey an n^{-3} law asymptotically as $n^{-2} \to 0$. We may exploit this fact to obtain a unified graphical representation of the various $1s$-ns and $1s$-np total Glauber cross section in e^--H and H^+-H collisions by plotting the normalized values of the cross sections. The considerations of the preceding paragraph then suggest that the normalization be made to the scaled asymptotic values of the cross sections.

We have plotted against v_i^2 the integrated Glauber cross sections for both electron and proton impact collisions after normalizing the cross sections for $n \geq 3$ states to the corresponding scaled (i.e., n cubed) asymptotic values:

$$\lim_{n\to\infty} \bar{\sigma}(1s \to ns, np) = \lim_{n\to\infty} n^3 \sigma(1s \to ns, np) .$$

The H^+ impact results are normalized at 100 keV, while the e^- impact results are normalized at 100 eV. For either process, each of the electron and proton impact curves for various n show a complete superposition above some energy value. For H^+ impact curves, this occurs above approximately 75 keV ($v_i^2 = 3$ a.u.). For e^- impact curves, the superposition occurs above nearly 65 eV ($v_i^2 \simeq 5$ a.u.) in case of $1s$-ns excitations and above about 50 eV ($v_i^2 \simeq 4$ a.u.) in case of $1s$-np excitations. The results are shown in Fig. 5. As expected, the e^- and H^+ impact curves for $1s$-ns ex-

citations are seen to approach each other at high incident velocity, while those corresponding to $1s$-np excitations coincide above about $v_i^2 = 16$ a.u. It should be noted that Fig. 5 gives the exact scaled asymptotic cross sections for $1s$-ns and $1s$-np excitations in e^--H and H^+-H collisions, while for any discrete state $n \geq 3$, the cross sections shown are only the normalized values.

The curves of Fig. 5 may be used to furnish the relative values of the Glauber cross sections at any two energies for arbitrary $1s$-ns or $1s$-np excitation to $n \geq 3$ states. Furthermore, since the Glauber and Born cross sections converge at high energies (see Figs. 1 and 2), a Born calculation for any given $1s$-ns or $1s$-np excitation at high energy (cf. Ref. 24) would then suffice for an estimation of the absolute Glauber cross sections for that particular n excitation at lower energies.

To illustrate the procedure, we consider the H^+ impact $1s$-ns curve of Fig. 5. The normalized cross sections at $v_i^2 = 8$ and 16 a.u. are read as 0.197 and 0.106 in units of πa_0^2. The absolute value of the scaled (n cubed) Born cross sections for $1s$-$4s$ excitation at $v_i^2 = 16$ a.u. ($E = 400$ keV) amounts to $0.128\pi a_0^2$ (Ref. 18). This may also be taken as the value predictable by the Glauber method, for the Glauber and Born curves are coincident at 400 keV (see Fig. 3). Then we obtain for the absolute value of the scaled Glauber cross sections at 200 keV for $1s$-$4s$ excitation in H^+-H collision:

$$[\sigma(1s \rightarrow 4s)]_{200\,\mathrm{keV}} = 0.128(0.197/0.106)\pi a_0^2$$

which comes out to be $0.024\pi a_0^2$ and differs by only 4% from the exact Glauber value, $0.023\pi a_0^2$, as can be read from Table V.

ACKNOWLEDGMENT

The authors are thankful to Dr. S.C. Mukherjee, Indian Association for the Cultivation of Science, Calcutta, for his interest in the problem.

[1] I. C. Percival and D. Richards, Adv. At. Mol. Phys. 11, 1 (1975).
[2] N. Toshima, J. Phys. Soc. Jpn. 43, 610 (1977).
[3] N. C. Sil, B. C. Saha, H. P. Saha, and P. Mandal, Phys. Rev. A 19, 655 (1979); C. Mitra, N. Roy, and N. C. Sil, J. Phys. B 11, 1807 (1978); N. C. Sil and S. K. Sur, *Abstracts of the Papers of the Eleventh International Conference on the Physics of Electronic and Atomic Collisions, Kyoto, Japan*, 1979 (The Society for Atomic Collision Research, Japan, Kyoto, 1979), p. 128.
[4] R. J. Glauber, in *Lectures in Theoretical Physics*, edited by W. E. Brittin *et al.* (Interscience, New York, 1959), Vol. 1, p. 315.
[5] E. Gerjuoy and H. K. Thomas, Rep. Prog. Phys. 37, 1345 (1974); F. W. Byron, Jr., and C. J. Joachain, Phys. Rep. 34C, 233 (1977).
[6] V. Franco, Phys. Rev. Lett. 20, 709 (1968).
[7] B. K. Thomas and V. Franco, Phys. Rev. A 13, 2004 (1976).
[8] J. T. Park, J. E. Aldag, J. L. Peacher, and J. M. George, Phys. Rev. Lett. 40, 1646 (1978); Phys. Rev. A 21, 751 (1980).
[9] A. S. Ghosh and N. C. Sil, Indian J. Phys. 43, 490 (1969); 44, 153 (1970); A. S. Ghosh, P. Sinha, and N. C. Sil, J. Phys. B 3, L58 (1970).
[10] H. Tai, R. H. Bassel, E. Gerjuoy, and V. Franco, Phys. Rev. A 1, 1819 (1970).
[11] A. S. Ghosh and N. C. Sil, J. Phys. B 4, 836 (1971).
[12] V. Franco and B. K. Thomas, Phys. Rev. A 4, 945 (1971).
[13] B. K. Thomas and E. Gerjuoy, J. Math. Phys. (N.Y.) 12, 1567 (1971).
[14] S. Kumar and M. K. Srivastava, Pramana 9, 87 (1977).
[15] S. K. Sur and N. C. Sil, Phys. Lett. 74A, 48 (1979).
[16] L. I. Schiff, *Quantum Mechanics*, 3rd ed. (McGraw-Hill, New York, 1968), p. 93.
[17] See, for example, H. Margenau and G. M. Murphy, *The Mathematics of Physics and Chemistry* (Van Nostrand, New York, 1955), Vol. 1, pp. 127 and 129; and also W. Magnus, F. Oberhettinger, and R. P. Soni, *Formulas and Theorems for the Special Functions of Mathematical Physics* (Springer, New York, 1966), pp. 240 and 244. It should be noted that the Laguerre polynomial defined by Schiff (Ref. 16) differs in normalization from the conventional definition (cf., Ref. 28).
[18] B. C. Saha, H. P. Saha, and N. C. Sil, J. Phys. Soc. Jpn. 47, 1634 (1979).
[19] R. F. Syms, M. R. C. McDowell, L. A. Morgan, and V. P. Myerscough, J. Phys. B 8, 2817 (1975).
[20] A. H. Mahan, A. Gallaher, and S. Smith, Phys. Rev. 13, 156 (1976).
[21] M. R. C. McDowell, L. A. Morgan, and V. P. Myerscough, J. Phys. B 6, 1435 (1973).
[22] M. R. Flannery and K. J. McCann, J. Phys. B 7, L522 (1974).
[23] D. Bayne and P. H. Heenen, J. Phys. B 7, 928 (1974).
[24] H. P. Saha and B. C. Saha, Phys. Lett. 69A, 180 (1978); P. K. Roy, B. C. Saha, and N. C. Sil, J. Phys. B (to be published).
[25] D. Bayne and P. H. Heenen, J. Phys. B 6, 105 (1973).
[26] R. Shakeshaft, Phys. Rev. A 18, 1930 (1978).
[27] T. J. Morgan, J. Gedder, and H. Gilbody, J. Phys. B 6, 2118 (1973).
[28] I. S. Gradshteyn and I. M. Ryzhik, *Tables of Integrals, Series and Products*, 4th ed. (Academic, New York, 1965).